Journal of Theoretical and Applied Mechanics, Sofia, Vol.52 (2022) pp. 335-350
COMBINED MECHANICAL FIELDS

DYNAMIC NANO-CRACKS INTERACTION IN GRADED MAGNETOELECTROELASTIC SOLID

TSVIATKO V. RANGELOV[1*], YONKO D. STOYNOV[2], PETIA S. DINEVA[3]

[1]*Institute of Mathematics and Informatics, Bulgarian Academy of Sciences, Sofia 1113, Bulgaria*
[2]*Faculty of Applied Mathematics and Informatics, Technical University, Sofia 1000, Bulgaria*
[3]*Institute of Mechanics, Bulgarian Academy of Sciences, Sofia 1113, Bulgaria*

[Received: 20 November 2021. Accepted: 05 April 2022]

doi: https://doi.org/10.55787/jtams.22.52.4.335

ABSTRACT: Dynamic fracture behaviour of multiple anti-plane nano-cracks in infinite functionally graded magnetoelectroelastic (MEE) solid under excitation of time-harmonic SH-wave is studied. The applied approach is based on the non-hypersingular traction based boundary integral equation method (BIEM) for the graded bulk MEE solid extended with the non-classical boundary conditions and the localized constitutive law for the MEE matrix-nanocrack interface within the framework of the Gurtin-Murdoch theory. The formulation allows for an exponential variation of the material properties in an arbitrary direction. The boundary integral equation (BIE) system is treated by using the frequency dependent fundamental solution derived analytically by Fourier transforms. The numerical solution provides displacements and tractions at any point in the infinite graded solid as well as the generalized crack opening displacements from which the generalized stress concentrations are determined. Simulations for different nano-cracks configurations such as collinear, parallel or nanocracks in arbitrary position to each other are presented and discussed. They demonstrate among others the MEE coupling, the frequency dependent shielding and amplification effects resulting from nano-cracks interaction and reveal the sensitivity of the stress concentration factors to the complex influence of wave-crack and crack-crack interactions, existence of material gradient and surface elasticity effects.

KEY WORDS: Anti-plane multiple nano-cracks; Functional graded material; Magnetoelectroelasticity, Gurtin-Murdoch model, Stress Concentration Field, Boundary integral equation method.

*Corresponding author e-mail: rangelov@math.bas.bg

1 INTRODUCTION

The main feature of magnetoelectroelastic (MEE) composite materials that makes them attractive for use in numerous modern multifunctional technical implementations such as microwave devices, sensors, transducers, filters, memory elements, energy harvesters, batteries, etc. is their capacity to convert energy among the magnetic, electric and mechanical fields. The triple energy conversions have facilitated MEE materials to exhibit excellent multifunctionality. A coupled electrical and magnetic phenomenon is realized via elastic interaction. The magnetic phase changes its shape magnetostrictively when a magnetic field is applied to a composite. The strain is then passed along to the piezoelectric phase, resulting in an electric polarization. In the last years MEE nanostructures have become an extremely important topic, since they, especially magneto-electric thin films, are easy to on-chip integration, which is a prerequisite for incorporation into microelectronic devices. Additionally, in the last years the next new class of smart MEE materials appear and they are so called functionally graded materials (FGM) with continuously varying properties that have significant advantages over discretely layered composites. These modern functionally graded MEE composites are very attractive also for nano-sensors, nano-actuators and nano-transducers. Due to their inherent brittleness, fracture behavior and reliability have to be evaluated. One of the key issues regarding the fast growing use of this class of smart FGM is related to understanding and modeling their fracture behavior under combined mechanical, electric and magnetic static, time-harmonic and impact loadings. As compared to the piezoelectric cases, relatively limited work has been done so far when it comes to analyze fracture phenomena in graded MEE materials. This is true with even greater force for continuously inhomogeneous functional graded nano-cracked MEE materials. A literature review for available in the literature results concerning dynamic fracture problems of graded MEE materials with cracks at macro and nano-level shows the following state. 2D dynamic fracture problems in graded MEE solids with macro-cracks are considered in [1–10]. One of the main thrusts of what is now known as nano-scale mechanics is the so called multi-scale approach, which aims at extending the range of classical continuum mechanics by bridging its basic theoretical principles with the effects observed at the molecular level. Along this direction we mention the pioneering work of [11, 12] who developed a general theoretical frame work to represent both surface and interface stresses. A review for dynamic fracture behaviour of piezoelectric and MME nano-composites in the frame of Gurtin and Murdoch model shows that few results are available. The only known result is in [13], where anti-plane elastodynamic problem for shear (SH) wave scattering by a single nano-crack in a homogeneous MEE plane is solved. [14] studied dynamic fracture behavior of an in-plane nano-crack in a

homogeneous piezoelectric plane under incident time-harmonic P or SV wave. Anti-plane dynamic problem of a finite exponentially inhomogeneous piezoelectric solid with a nano-crack is solved in [15]. To the authors knowledge there are no available results for static or dynamic fracture behaviour of multiple nano-cracks in graded MEE continua.

The main aim of this work is to solve 2D dynamic problem for scattering, diffraction and stress concentration in a graded MEE plane with multiple nano-cracks subjected to normal plane time-harmonic SH-wave by developing of a non-hypersingular traction based BIEM extended by the non-classical boundary condition derived in [11, 12] model. The paper is a continuation of our previous results in [13, 16] where we consider nanocracked homogeneous MEE material in the first one and exponentially inhomogeneous MEE media with a single nano-crack in the second one.

The paper is organized as follows: the statement of the problem and its reformulation by non-hypersingular traction boundary integral equations are given in Sect. 2 and Sect. 3 correspondingly. Numerical results are presented in Sect. 4, while concluding remarks are discussed in Sect. 5.

2 Problem statement

In a Cartesian coordinate system $Ox_1x_2x_3$ consider an infinite exponentially inhomogeneous transversely isotropic MEE plane $x_3 = 0$ subjected to incident time-harmonic with frequency ω and incident angle θ shear SH wave which is polarized along Ox_3 axis. Assume that MEE material shows hexagonal symmetry with respect to the axis Ox_3 and the poling axis is collinear with Ox_3 axis.

The only non-zero field quantities in the case of anti-plane strain state under consideration are:

i) mechanical field variables: out-of-plane mechanical displacement $u_3(x,\omega)$, stress components $\sigma_{13}(x,\omega)$, $\sigma_{23}(x,\omega)$ and strain components $s_{13}(x,\omega)$, $s_{23}(x,\omega)$, all dependent on coordinates $x = (x_1, x_2)$;

ii) electrical and magnetic field variables: in-plane components of the electric field $E_1(x,\omega)$, $E_2(x,\omega)$, electrical displacements $D_1(x,\omega)$, $D_2(x,\omega)$, magnetic induction $B_1(x,\omega)$, $B_2(x,\omega)$ and magnetic field $H_1(x,\omega)$, $H_2(x,\omega)$.

Material characteristics such as density $\rho(x)$, elastic shear stiffness $c_{44}(x)$, piezoelectric coupled coefficient $e_{15}(x)$, dielectric permittivity $\varepsilon_{11}(x)$, piezomagnetic parameter $q_{15}(x)$, magnetoelectric parameter $d_{11}(x)$ and magnetic permeability $\mu_{11}(x)$ are variables with respect to the position vector $x = (x_1, x_2)$. They are defined by

the inhomogeneous function $h(x) = e^{2\langle a,x\rangle}$ as follows:

$$
\begin{aligned}
(1) \qquad & \rho(x) = \rho^0 h(x), \;\; c_{44} = c_{44}^0 h(x), \;\; e_{15} = e_{15}^0 h(x), \;\; \varepsilon_{11} = \varepsilon_{11}^0 h(x), \\
& q_{15} = q_{15}^0 h(x), \;\; d_{11} = d_{11}^0 h(x), \;\; \mu_{11} = \mu_{11}^0 h(x),
\end{aligned}
$$

In the definition of function $h(x)$, the notation $\langle .,. \rangle$ is the scalar product in R^2, $a = (a_1, a_2)$ is the inhomogeneity vector with the following components $a_1 = |a| \cos\alpha$, $a_2 = |a| \sin\alpha$, $|a| = \sqrt{a_1^2 + a_2^2}$, α is the inhomogeneity direction, and ρ^0, c_{44}^0, e_{15}^0, ε_{11}^0, q_{15}^0, d_{15}^0, μ_{11}^0 are the reference material properties at $a = 0$, i.e., material properties of the homogeneous material.

The graded MEE plane contains N straight nano-cracks with boundaries S_k, $k = 1, 2, \ldots N$, see Fig. 1a. The number of nano-cracks and their geometrical configuration is arbitrary. The model of the k-th nano-crack is a blunt crack with a crack's root presented by a semi-elliptical shape with semi-major axis d_0 and semi-minor axis d, $d \le d_0$, see Fig. 1b. The perimeter of the crack is $|S| = 2(2c - 2d_0) + 4d_0 E(e)$, $d_0 = 0.0375c$, with a size c belonging to the interval $10^{-7}m - 10^{-10}m$, where $e = \sqrt{1 - (d/d_0)^2}$ and $E(e) = \int_0^{\pi/2} \sqrt{1 - e^2 \sin^2\varphi}\, d\varphi$ is a complete elliptic integral of second kind, see [17]. If $d = d_0$ the blunt nano-crack is with a crack's root presented by semi-circular shape of radius d_0.

An illustrative examples will be considered two nano-cracks in the following mutual dispositions: (a) collinear cracks S and S_1; (b) parallel cracks S and S_2; (c) shifted nano-cracks S and S_3. We mark on Fig. 1a some corner points on the cracks in order to define the distance between them in the numerical examples: $\mathrm{dist}(S, S_1) = |C - C_1|$, $\mathrm{dist}(S, S_2) = |C - C_2|$ and $\mathrm{dist}(S, S_3) = |C - C_3|$.

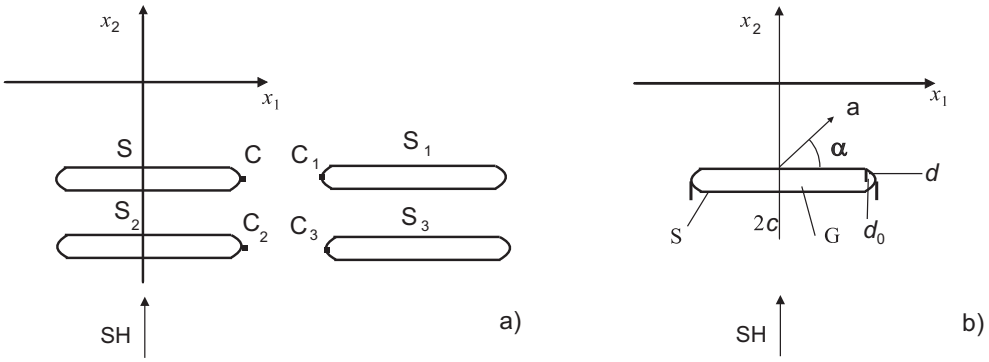

Fig. 1: A graded MEE plane subjected to normal incident time-harmonic SH- wave. a) Multiple blunt nano-cracks: collinear S, S_1, parallel S, S_2, shifted S, S_3 ; b) Reference model of a single blunt nano-crack S.

Fracture mechanics considers the crack front profile as an infinite sharp, where the elastic and elasto-plastic crack-tip zones are well established. In reality the crack-tips are not ideally sharp, but blunt with a curvature radius in the order of microns or nanometers. In [18] is shown that the surface elasticity effect is localized at the crack-tip. The stresses obtained via the atomic models are in a good agreement with the predictions of linear fracture mechanics except in a very small vicinity of the crack tip, where the effect of surface elastic energy should be taken into account.

The compact form of the constitutive equations in the plane $x_3 = 0$ is obtained by introducing the generalized field quantities described below, see [19, 20].

$$\sigma(x,\omega)_{iK} = C_{iKJl}(x)u_{J,l}(x,\omega), \quad x \in R^2\backslash\Gamma, \text{ or } x \in R^2\backslash G, \tag{2}$$

where small indexes $i, l = 1, 2$, capital indexes $K, J = 3, 4, 5$, comma denotes partial differentiation and summation in repeating indexes is assumed. The generalized field variables are defined as follows:

- generalized displacement is $u_J(x,\omega) = (u_3(x,\omega), \phi(x,\omega), \varphi(x,\omega))$;
- generalized stress tensor is $\sigma_{iJ}(x,\omega) = (\sigma_{i3}(x,\omega), D_i(x,\omega), B_i(x,\omega))$ and
- generalized elasticity tensor is $C_{iKJl}(x)$ with the following components:

$$C_{i33l}(x) = \begin{cases} c_{44}(x), & i = l \\ 0, & i \neq l \end{cases}, \qquad C_{i34l}(x) = C_{i43l}(x) = \begin{cases} e_{15}(x), & i = l \\ 0, & i \neq l \end{cases},$$

$$C_{i35l}(x) = C_{i53l}(x) = \begin{cases} q_{15}(x), & i = l \\ 0, & i \neq l \end{cases} \qquad C_{i44l}(x) = \begin{cases} -\varepsilon_{11}(x), & i = l \\ 0, & i \neq l \end{cases},$$

$$C_{i45l}(x) = C_{i54l}(x) = \begin{cases} -d_{11}(x), & i = l \\ 0, & i \neq l \end{cases}, \quad C_{i55l}(x) = \begin{cases} -\mu_{11}(x), & i = l \\ 0, & i \neq l \end{cases}$$

The kinematics relations under assumption of small displacements and electric ϕ and magnetic φ field-potentials relations under quasi-static approximation, see [20] are the next group of the governing equations:

$$\begin{aligned} s_{i3}(x,\omega) &= u_{3,i}(x,\omega), \\ E_i(x,\omega) &= -\phi_{,i}(x,\omega), \\ H_i(x,\omega) &= -\varphi_{,i}(x,\omega), \quad \text{and} \quad i = 1, 2. \end{aligned} \tag{3}$$

The dynamic equilibrium equation in the case there are no body force and free electric and magnetic volume charges is given below, having in mind Eqs. (2), (3).

$$\sigma_{iK,i} + \rho_{KJ}\omega^2 u_J = 0, \quad i = 1, 2, J, K = 3, 4, 5, \tag{4}$$

where $\rho_{KJ}(x) = \begin{cases} \rho(x), & K = J = 3, \\ 0, & K, J = 4 \text{ or } 5. \end{cases}$.

For simplicity and if there is no misunderstanding we will omit the arguments of the functions. The following assumptions are made: (a) the bulk material is transversely isotropic MEE one describing via the constitutive equation (2); (b) the interface S_k between the k-th nano-crack and the matrix material is considered as an infinitely thin elastic isotropic layer with own surface elastic shear coefficient μ^S and the following constitutive equation describes its behaviour $\sigma^S_{l3} = c^S_{44} s^S_{l3} = \mu^S \dfrac{\partial u^S_3}{\partial l}$, here l is the tangential vector along the interface S_k and $\frac{\partial u^S_3}{\partial l}$ is the tangential derivative of the mechanical displacement u^S_3; (c) the infinitely thin interface layer S_k is coherent and no atomic bonds are broken along it. Along coherent boundary which is perfect bonded, the surface mechanical strain in tangential direction with respect to the interface boundary is equal to the associated tangential strain inside the matrix, i.e. $s^S_{l3} = s^M_{l3}$.

The cracks are assumed to be electrically and magnetic impermeable and in this case the electric and magnetic field inside the cracks is ignored and they may be thought as a low-capacitance medium with electric and magnetic potential jumps $\Delta\phi = \phi^+ - \phi^-$ and $\Delta\varphi = \varphi^+ - \varphi^-$. The generalized traction vector over S_k is defined as $t_J = (t_3, t_4, t_5)$, where $t_3 = \sigma_{i3} n_i, \quad n = (n_1, n_2)$ is the normal vector on $S_k, \quad t_4 = D_n, \quad t_5 = B_n$. The boundary conditions for the normal component of the electric displacement and magnetic induction along the nano-crack S_k are $D_n = 0$ and $B_n = 0$, while the boundary condition for the mechanical stress satisfies the non-classical boundary condition, derived in the frame of the [11, 12] theory

$$\sigma^M_{n3} = t^M_3 = t_3 = -\frac{\partial \sigma^S_{l3}}{\partial l} = -\mu^S \frac{\partial^2 u_3}{\partial l^2}, \quad x \in S_k, \quad k = 1, \ldots, N. \tag{5}$$

Note that at zero surface elastic properties, i.e., $\mu^S = 0$, the boundary condition (5) degenerates to the classical boundary condition as $t_3 = 0$.

The total wave field $u_J, \quad \sigma_{iJ}$ in the graded MEE plane can be written as a sum of the incident $u^{in}_J, \quad \sigma^{in}_{iJ}$ and the scattered $u^{sc}_J, \quad \sigma^{sc}_{iJ}$ wave fields, i.e., $u_J = u^{in}_J + u^{sc}_J$ and $\sigma_{iJ} = \sigma^{in}_{iJ} + \sigma^{sc}_{iJ}$. The generalized displacement and stress of the incident SH wave propagating in a MEE continuum is presented in [8]. The scattered by the cracks wave field is unknown and has to be determined.

Finally, the solution for the total wave field of the defined BVP satisfies the governing Eq. (4), the boundary condition (5) for the k-th blunt nano-crack and the Sommerfeld's radiation condition for the scattered wave at infinite.

The computation of the generalized normalized stress concentration factor (GSCF) close to the interface S of a blunt nano-crack at point $(\pm x_1, 0)$ is proceed with the formulae

$$
\begin{aligned}
F_{III}((x_1,0),\omega) &= \frac{t_3((x_1,0),\omega)\sqrt{2\pi(x_1 \mp c)}}{t_3^{in}((x_1,0),\omega)}, \quad |x_1| > c,\\
F_E((x_1,0),\omega) &= \frac{E_n((x_1,0),\omega)\sqrt{2\pi(x_1 \mp c)}}{t_3^{in}((x_1,0),\omega)}, \quad |x_1| > c,\\
F_H((x_1,0),\omega) &= \frac{H_n((x_1,0),\omega)\sqrt{2\pi(x_1 \mp c)}}{t_3^{in}((x_1,0),\omega)}.
\end{aligned} \tag{6}
$$

Here

$$
\begin{aligned}
E_n &= M_{21}t_3((x_1,0),\omega) + M_{22}t_4((x_1,0),\omega) + M_{23}t_5((x_1,0),\omega),\\
H_n &= M_{31}t_3((x_1,0),\omega) + M_{32}t_4((x_1,0),\omega) + M_{33}t_5((x_1,0),\omega),
\end{aligned}
$$

$\{M_{ij}\}$ are sub-determinants of the matrix $M = \begin{pmatrix} c_{44}^0 & e_{15}^0 & q_{15}^0 \\ e_{15}^0 & -\varepsilon_{11}^0 & -d_{11}^0 \\ q_{15}^0 & -d_{11}^0 & -\mu_{11}^0 \end{pmatrix}$, see [8, 10].

In the figures of Section 4 we plot the normalized GSCFs $F_{III}^* = |F_{III}/\sqrt{\pi c}|$, $F_E^* = |F_E/\sqrt{\pi c}|$, $F_H^* = |F_H/\sqrt{\pi c}|$.

3 Non-Hypersingular Traction Boundary Integral Equation Method for Solution of the Problem

The BIEM is an attractive candidate for modelling of wave propagation in heterogeneous media with coupled properties because of certain advantages, discussed in details in [21].

However, it is well known that the conventional displacement BIE formulation degenerates for crack problems and it cannot be directly applied to them, see [22, 23]. Generally there are several methods to overcome this difficulty and among them is the non-hypersingular traction based BIEM proposed for elastic isotropic and homogeneous solids in [24]. The derivation of the mentioned approach is done here via combine usage of the two-state conservation integral of elastodynamics and the frequency-dependent fundamental solution for anti-plane wave motion in 2D exponentially graded MEE plane, following [8, 16].

In the considered case of multiple blunt nano-cracks the formulated above BVP is presented by the following system of integro-differential equations along the interface between the MEE matrix and the nano-cracks:

$$
\begin{aligned}
\gamma_{RJ}(t_R^{in}(x,\omega) - t_R^M(x,\omega)) &= C_{iJKl}(x)n_i(x)\\
&\times \sum_{k=1}^{N} \int_{S_k} \Big[\Big(\sigma_{\eta PK}^*(x,y,\omega) u_{P,\eta}^{sc,k}(y,\omega) - \rho_{QP}\omega^2 u_{QK}^*(x,y,\omega) u_P^{sc,k} \Big) \delta_{\lambda l}\\
&\quad - \sigma_{\lambda PK}^*(x,y,\omega) u_{P,l}^{sc,k}(y,\omega) \Big] n_\lambda(y) dS_y, \quad x \in \cup_{k=1}^{N} S_k.
\end{aligned} \tag{7}
$$

Here γ_{RJ} is the jump term depending on the local geometry at the source point x, $x = (x_1, x_2)$ and $y = (y_1, y_2)$ are the position vectors of the source and field points, u^*_{QK} is the fundamental solution of Eq. (4), i.e., Eq. (4) with right hand side $-\delta(x-y)I_3$, where $\delta(x-y)$ is Dirac's delta function and I_3 is unit 3×3 matrix. Symbol $\delta_{\lambda l}$ is the Kronecker symbol, $\sigma^*_{iJQ} = C_{iJMl}u^*_{MQ,l}$. The fundamental solution u^*_{QK} is derived analytically by Fourier transform following the steps: (i) First, application of the smooth functional transform $u^*_{KM} = e^{-\langle a,x\rangle}U^*_{KM}$ to both sides of Eq. (4) with right hand side $-e^{-\langle a,\xi\rangle}\delta_{KM}\delta(x,\xi)$, aiming to obtain partial differential equation with constant coefficients with respect to U^*_{KM}; (ii) The second step is an application of Fourier transform to equation with constant coefficients and its solution, see [25], in analytical form; (iii) The third step deals with the application of inverse Fourier transform and analytical derivation of the function U^*_{KM}; (iv) Final step presents fundamental solutions u^*_{KM} for equation of motion in an exponentially graded MEE continua. The derived fundamental solution is a 3×3 matrix-valued function and is listed below. It is different from the one derived by Radon transform in [8] and applied for numerical simulations in [16].

The wave number is $k = \sqrt{\dfrac{\rho^0\omega^2}{a_0} - |a|^2}$ with $a_0 = \overline{c}^0_{44} + \dfrac{\overline{e}^{02}_{15}}{\overline{\varepsilon}^0_{11}}$, $\overline{c}^0_{44} = c^0_{44} + \dfrac{q^{02}_{15}}{\mu^0_{11}}$, $\overline{e}^0_{15} = e^0_{15} - \dfrac{d^0_{11}q^0_{15}}{\mu^0_{11}}$, $\overline{\varepsilon}^0_{11} = \varepsilon^0_{11} - \dfrac{d^{02}_{11}}{\mu^0_{11}}$ and let us introduce the notations

$$A = \frac{\mu^0_{11}e^0_{15} - q^0_{15}d^0_{11}}{\mu^0_{11}\varepsilon^0_{11} - (d^0_{11})^2}, \quad B = \frac{q^0_{15}\varepsilon^0_{11} - e^0_{15}d^0_{11}}{\mu^0_{11}\varepsilon^0_{11} - (d^0_{11})^2}.$$

The critical (cut-off) frequency is defined as $\omega_0 = |a|\sqrt{a_0/\rho^0}$ and $\omega_0 > 0$ for $a \neq 0$. In the case $\omega > \omega_0$ corresponds to the mechanical case of wave propagation and then the fundamental solution has the form:

$$u^*(x,y,\omega) = -\frac{e^{-\langle a,x+y\rangle}}{2\pi a_0}\begin{pmatrix} 1 & A & B \\ A & A^2 & AB \\ B & AB & B^2 \end{pmatrix} K_0(-ikr)$$

$$+\frac{e^{-\langle a,x+y\rangle}}{2\pi}\begin{pmatrix} 0 & 0 & 0 \\ 0 & -\dfrac{1}{\overline{\varepsilon}^0_{11}} & \dfrac{d^0_{11}}{\overline{\varepsilon}^0_{11}\mu^0_{11}} \\ 0 & \dfrac{d^0_{11}}{\overline{\varepsilon}^0_{11}\mu^0_{11}} & -\left(\dfrac{d^{02}_{11}}{\overline{\varepsilon}^0_{11}\mu^{02}_{11}} + \dfrac{1}{\mu^0_{11}}\right) \end{pmatrix} K_0(|a|r),$$

where $K_0(z)$ is Kelvin function, see [17] and $r = \sqrt{(x_1-y_1)^2 + (x_2-y_2)^2}$.

After discretization and collocation procedure applied to Eq. (7), the defined problem transforms to a system of algebraic equations with respect to the unknown scattered displacements $u_J^{sc,k}$ along the k-th crack line S_k. Note, that the obtained after discretization integrals are at least Cauchy principal value integrals.

Once the solution of the system of BIEs (7) is known for a fixed frequency ω, the displacement and stress of the scattered field and by this the total field in the whole MEE plane can be determined via the representation formulae

$$(8)\quad u_J^{sc}(x,\omega) = -\sum_{k=1}^{N}\Big\{\int\limits_{S_k}\sigma_{iMJ}^{*}(x,y,\omega)u_M^{sc,k}(y,\omega)n_i(y)dS_k,\quad x\notin\cup_{k=1}^{N}S_k,$$

$$(9)\quad t_J^{sc}(x,\omega) = -C_{iJKl}(x)n_i(x)\sum_{k=1}^{N}\Big\{\int\limits_{S_k}\Big[(\sigma_{\eta PK}^{*}(x,y,\omega)\Delta u_{P,\eta}^{sc,k}(y,\omega) - \rho_{QP}\omega^2 u_{QK}^{*}(x,y,\omega)u_P^{sc,k})\delta_{\lambda l} - \sigma_{\lambda PK}^{*}(x,y,\omega)u_{P,l}^{sc,k}(y,\omega)\Big]n_\lambda(y)d\Gamma_y\Big\},\quad x\notin\cup_{k=1}^{N}S_k.$$

4 Numerical Results

The program code using Mathematica 6.0, see [26], has been created for solution of the above described problem. The numerical results are for magnetoelectroelastic composite $BaTiO_3/CoFe_2O_4$. It is assumed that the material constants k_c^0 of the composite made of $BaTiO_3$ as an inclusion with reference material properties k_i^0 and $CoFe_2O_4$ as a matrix with reference material properties k_m^0 are defined by the usage of the formula $k_c^0 = 0.5(k_i^0 + k_m^0)$ proposed in [27]. In sum the used reference constants are: $c_{44}^0 = 44.15$ GPa, $e_{15}^0 = 11.6$ C/m^2, $\varepsilon_{11}^0 = 5.64\times10^{-10}$ C^2/Nm^2, $q_{15}^0 = 550$ N/Am, $\mu_{11}^0 = -590\times10^{-6}$ Ns^2/C^2, $\rho^0 = 6.65\times10^3$ kg/m^3. The magnetoelectric reference constant $d_{11}^0 = 5.2\times10^{-12}$ Ns/VC is chosen based on the micro-mechanical model proposed in [28]. The mesh of the blunt nano-crack with interface boundary S_k of length $|S_k| = 2.0428\times10^{-8}$ consists of 10 quadratic boundary elements, 8 along the flat parts $S_k^- \cup S_k^+$ and 2 along the left S_k^l and the right S_k^r elliptic edge.

The following normalized parameters are used: (a) normalized frequency defined as $\eta = c\omega\sqrt{a_0/\rho^0}$; (b) dimensionless inhomogeneity magnitude defined as $\beta = 2c|a|$; (c) dimensionless surface parameter defined as $s = \dfrac{\mu^S}{2c_{44}^0 dd_s}$ with μ^S=6.091 N/m. The values of μ^S are taken from the literature, see [29] and they are in the interval $[-10, 10]$ N/m. The parameter d_s is the curvature radius in the quarter point–boundary elements (QP-BE) used for adequately modelling the crack-tip zones. The

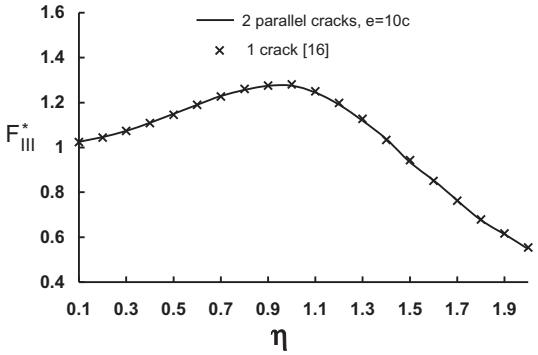

Fig. 2: Comparison between SCF F_3^* for one blunt nano crack S with $s = 0, \beta = 0$ in [16] and SCF F_3^* for two parallel blunt nano cracks S, S_1 with $s = 0, \beta = 0$ at distance $e = 10c$ in a cracked graded MEE plane under normal incident SH wave.

radius of curvature d_s in the QP-BEs increases proportionally when the blunt nano-crack approaches the line crack geometry. Conversely, when the value of surface parameter decreases to 0, we recover the case of the classical line crack and in this the SCFs F_{III}^*, F_E^*, F_H^* defined in equation (6) under the limit for $x_1 \to \pm c$ become SIFs K_{III}^*, K_E^*, K_H^*, see our earlier publication [14], where this was discussed in details.

The following values of the surface parameter s and ihomogeneity parameter β are considered in the parametric study: $s = 0.003; 0.8; -0.2$; and $\beta = 0; 0.6$.

To the authors' best knowledge, no results are currently available in the literature for the exponentially graded MEE plane containing two blunt nano-cracks. Due to this reason we verify our numerical scheme for multiple nano-cracks using the model of two collinear blunt nano-cracks situated in a homogeneous MEE plane under normal incident SH wave. The SCF results for two collinear cracks S and S_1, which are far away from each of other, i.e. when the distance e between them is $e = 10c$, should recover the SCF for a single crack S as far as the interaction between the two cracks is negligible on account of their large distance.

In order to illustrate this, we use the software code developed for the graded material, and then prescribe zero values to all coefficients relevant to the inhomogeneity. Fig. 2 compares the following frequency-dependent solutions of different BVPs in the case of normal time-harmonic SH-wave: (a) the authors' solution for normalized SCF F_{III}^* at the right crack-tip of a single blunt nano-crack with surface parameter $s = 0$ in a homogeneous MEE plane, see [16]; (b) the solution for normalized SCF F_{III}^* at the right crack-tip of the blunt nano-crack S, located in a graded MEE plane with inhomogeneity magnitude $\beta = 0$ at fixed surface parameter $s = 0$ and fixed

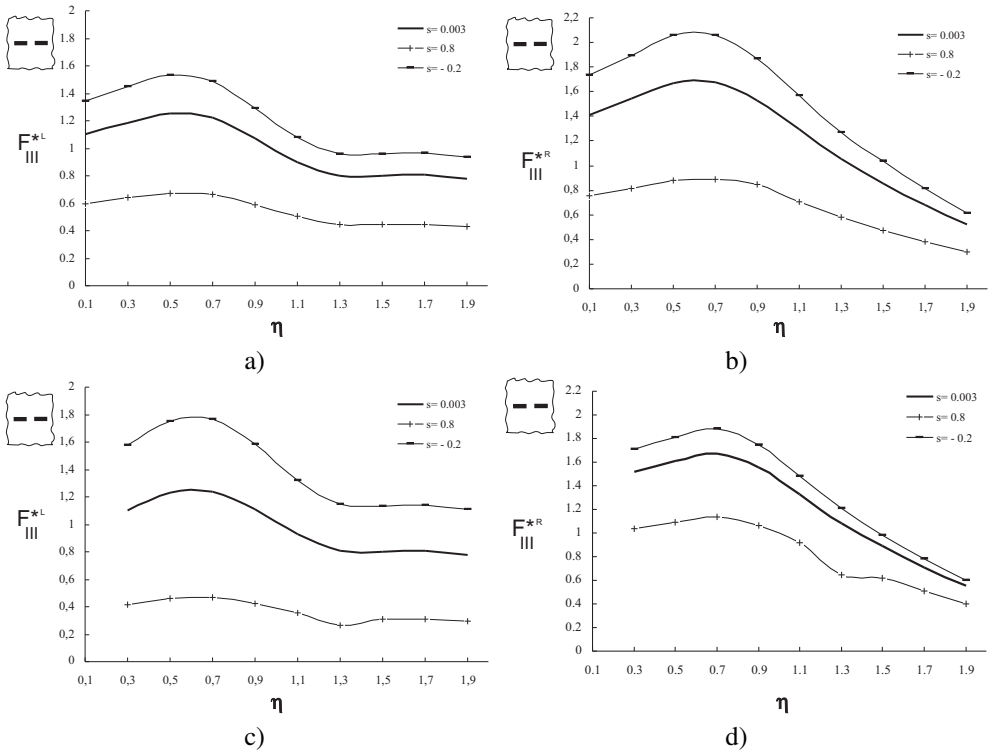

Fig. 3: Mechanical SCFs at the left (Figs. 3a, 3c) and right (Figs. 3b, 3d) crack-tip of the reference nanocrack S which is at a distance $e = 1.25c$ from its collinear nanocrack S_1 versus non-dimensional frequency η of normal incident SH-wave propagating in a graded MEE plane with inhomogeneity direction $\alpha = 0$, inhomogeneity magnitude $\beta = 0$ (homogeneous case) in Figs. 3a, b and $\beta = 0.6$ (graded material) in Figs. 3c, d. Results are for three different surface parameters $s = 0.003; 0.8; -0.2$.

distance $e = 10c$ from its collinear blunt nano-crack S_1, see Fig. 1a. As can be seen in Fig. 2 the two solutions are almost identical. This means, the fixed mesh satisfies excellent solution accuracy of the problem under consideration and it will be used in all of the rest numerical simulations.

Figures 3–5 show mechanical, electric and magnetic SCFs at the left (Figs. a and c) and right (Figs. b and d) crack-tip of the reference nano-crack S which is at a distance $e = 1.5c$ from its collinear nano-crack S_1 versus non-dimensional frequency η of SH-wave propagating in a graded MEE plane with inhomogeneity direction $\alpha = 0$, inhomogeneity magnitude $\beta = 0$ (homogeneous case) in Figs. a, b and $\beta = 0.6$ (graded material) in Figs. c, d. Results are for three different surface elasticity parameters $s = 0.003; 0.8; -0.2$.

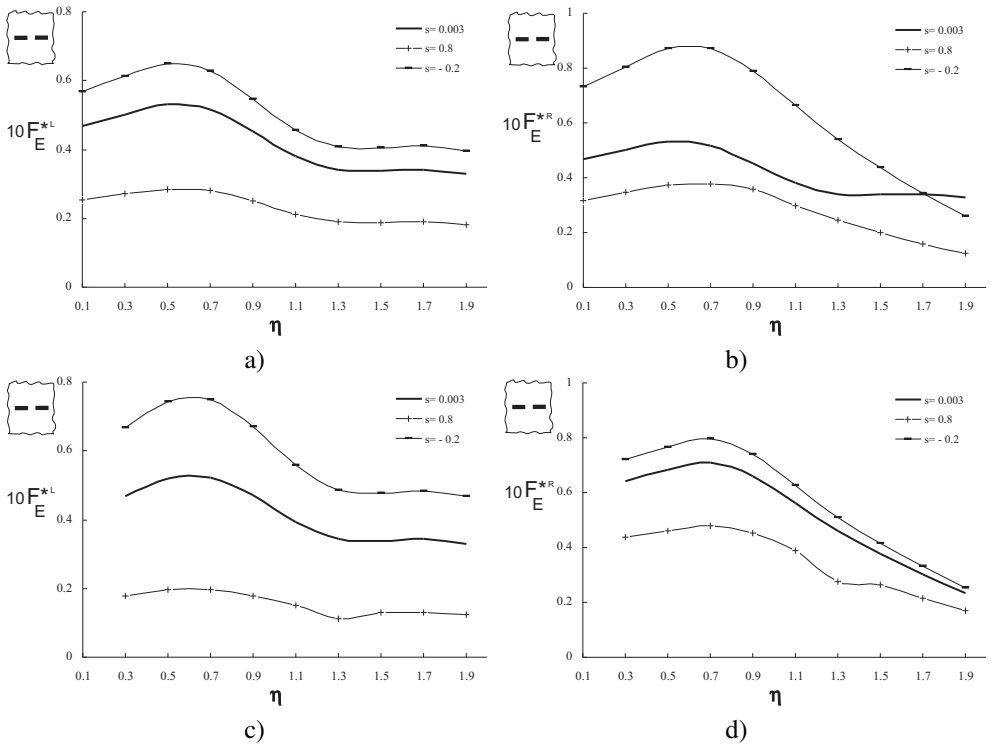

Fig. 4: Electric SCFs at the left (Figs. 4a, 4c) and right (Figs. 4b, 4d) crack-tip of the reference nanocrack S which is at a distance $e = 1.25c$ from its collinear nanocrack S_1 versus non-dimensional frequency η of normal incident SH-wave propagating in a graded MEE plane with inhomogeneity direction $\alpha = 0$, inhomogeneity magnitude $\beta = 0$ (homogeneous case) in Figs. 4a, b and $\beta = 0.6$ (graded material) in Figs. 4c, d. Results are for three different surface parameters $s = 0.003; 0.8; -0.2$.

Figure 6 illustrates the influence of the nano-cracks geometrical configuration on the frequency dependent stress concentration field. It draws mechanical SCFs at the right crack-tip of the reference nanocrack S versus non-dimensional frequency η of SH-wave propagating in a graded MEE plane with inhomogeneity direction α and inhomogeneity magnitude $\beta = 0.6$.

The following geometrical configurations are considered: (a) two collinear nano-cracks S and S_1 at distance $e = \text{dist}(S, S_1) = 1.25c$, see Figure 6a; (b) two parallel nano-cracks S and S_2 with distance $e = \text{dist}(S, S_2) = 1.25c$, see Figure 6b; (c) two shifted nano-cracks S and S_3, see Figure 6c with distance $e = \text{dist}(S, S_3) = 1.25\sqrt{2}c$. Figure 6 reveals the role of the geometrical disposition in the case of the multiple cracks. Amplification effect is visible in the case of parallel cracks (Fig. 6b),

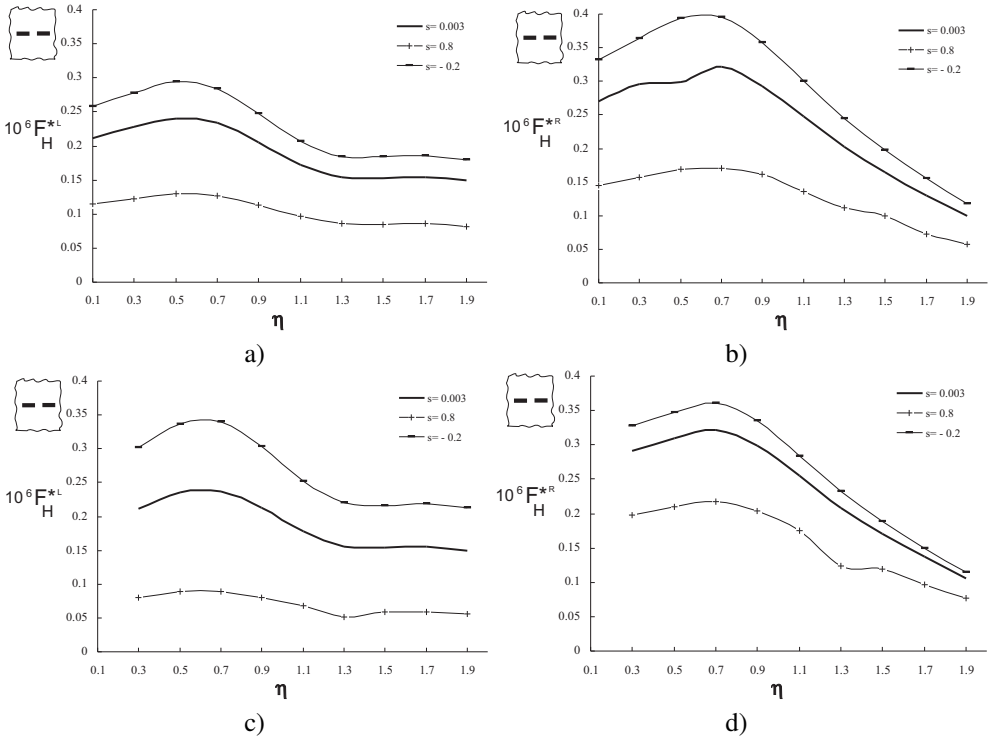

Fig. 5: Magnetic SCFs at the left (Figs. 5a, 5c) and right (Figs. 5b, 5d) crack-tip of the reference nanocrack S which is at a distance $e = 1.25c$ from its collinear nanocrack S_1 versus non-dimensional frequency η of normal incident SH-wave propagating in a graded MEE plane with inhomogeneity direction $\alpha = 0$, inhomogeneity magnitude $\beta = 0$ (homogeneous case) in Figs. 5a, b and $\beta = 0.6$ (graded material) in Figs. 5c, d. Results are for three different surface parameters $s = 0.003; 0.8; -0.2$.

while shielding phenomenon occurs in the case of shifted cracks, shown in Fig. 6c.

All the figures illustrate the frequency dependent shielding and amplification effects resulting from nano-cracks interaction and reveal the sensitivity of the stress concentration factors to the hybrid play of the following key factors: wave-crack and crack-crack interactions, existence of material gradient and surface elasticity, coupling between elastic, magnetic and electric fields.

5 Conclusion

Two dimensional dynamic anti-plane multiple nanocracks problem of a functionally graded MEE solid is solved in the frequency domain by means of non-hypersingular traction BIEM. The material properties vary exponentially in an arbitrary direction.

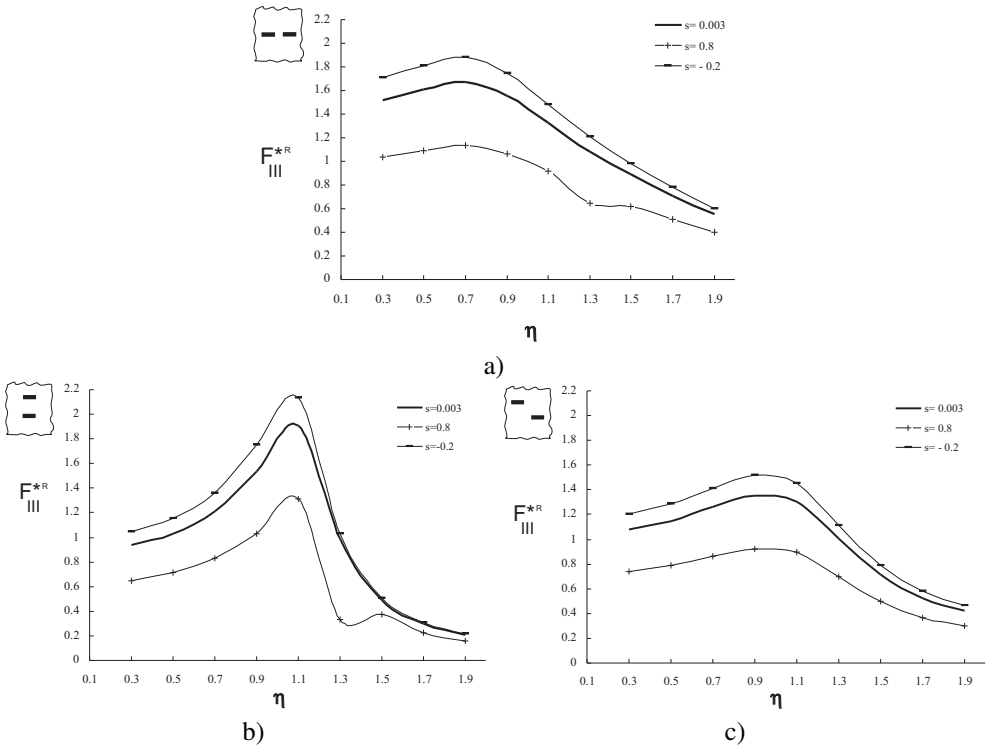

Fig. 6: Mechanical SCFs at the right crack-tip of the reference nanocrack S versus non-dimensional frequency η of normal incident SH-wave propagating in a graded MEE plane with inhomogeneity direction $\alpha = 0$ and inhomogeneity magnitude $\beta = 0.6$. The following geometrical configurations are considered: (a) two collinear nano-cracks S and S_1 at distance $e = 1.25c$, see Fig. 3d; (b) two parallel nano-cracks S and S_2 with distance $e = 1.25c$; (c) two shifted nano-cracks S and S_3 with distance $e = 1.25\sqrt{2}c$.

Numerical examples for two cracks in a plane under time-harmonic SH-wave are solved. The general conclusion from the simulations is that the dynamic stress field is a complex result of the dynamic load (its type and characteristics), the MEE material with its specific peculiarities like anisotropy, inhomogeneity, electro-magneto-mechanical coupling and the geometry of the cracks scenario (multiple cracks, crack-tip position). Numerical results demonstrate that the mechanical, the electric and the magnetic SCF are sensitive to the type, direction and magnitude of the material inhomogeneity, to the frequency of the applied load and to the relation between the magnitude of the gradient parameter and the crack size. Additionally, they are in-

fluenced strongly by the cracks interaction, surface elasticity and geometry of the nano-cracks system.

ACKNOWLEDGEMENT

The first and the third authors were partially supported by the Bulgarian National Science Fund, contract No КП-06-Н57/3/15.11.2021 and also by Grant No BG05M2OP001–1.001–0003, financed by the Science and Education for Smart Growth Operational Program (2014–2020) in Bulgaria and co-financed by the European Union through the European Structural and Investment Funds.

REFERENCES

[1] P.W. ZHANG, Z.G. ZHOU, AND B. WANG (2007) Dynamic behaviour of two collinear interace cracks between two dissimilar functionally graded piezoelectric/piezomagnetic material strips. *Applied Mathematics and Mechanics* **28** 615-625.

[2] P.W. ZHANG, Z.G. ZHOU, L.Z. WU (2008) Behaviour of three parallel non-symmetric mode III cracks in a functionally graded material plane. *Journal of Mechanical Engineering Science* **222** 2311-2330.

[3] J. LIANG (2008) The dynamic behaviour of two parallel symmetric cracks in functionally graded piezoelectric/piezomagnetic materials. *Archive of Applied Mechanics* **78** 443-464.

[4] Z.G. ZHOU, B. WANG (2008) An interface crack between two dissimilar functionally graded piezoelectric/piezomagnetic material half infinite planes subjected to the harmonic anti-plane shear stress waves. *International Journal of Applied Electromagnetics and Mechanics* **27** 117-132.

[5] Y.D. LI, K.Y. LEE (2008) Dynamic responses of a crack in a layered graded magneto-electroelastic sensor subjected to harmonic waves. *Acta Informatica* **204** 217-234.

[6] W. FENG AND R. SU (2006) Dynamic internal crack problem of a functionally graded magneto-electro-elastic strip. *International Journal of Solids and Structures* **43** 5196-5216.

[7] W. FENG, R. SU (2007) Dynamic fracture behaviors of cracks in a functionally graded magneto-electro-elastic plate. *European Journal of Mechanics; A/Solids* **26** 363-379.

[8] T. RANGELOV, Y. STOYNOV, P. DINEVA (2011) Dynamic fracture behavior of functionally graded magnetoelectroelastic solids by BIEM. *International Journal of Solids and Structures* **48** 2987-2999.

[9] J. SLADEK, V. SLADEK, P. SOLEK, E. PAN (2008) Fracture analysis of cracks in magnetoelectro-elastic solids by the MLPG. *Computational Mechanics* **42** 697714.

[10] J. SLADEK, V. SLADEK, P. SOLEK, C. ZHANG (2010) Fracture analysis in continuously nonhomogeneous magneto-electroelastic solids under a thermal load by the MLPG. *International Journal of Solids and Structures* **47** 13811391.

[11] M.E. GURTIN, A.I. MURDOCH (1975) A continuum theory of elastic material surfaces. *Archive for Rational Mechanics and Analysis* **57** 291-323.

[12] M.E. GURTIN, A.I. MURDOCH (1978) Surface stress in solids. *International Journal of Solids and Structures* **14** 431-440.

[13] Y. STOYNOV, P. DINEVA, T. RANGELOV (2019) Wave scattering and stress concentration in a magneto-electro-elastic plate with a nano-crack by boundary integral equations. *Journal of Theoretical and Applied Mechanics* **49** 203-223.

[14] T. RANGELOV, P. DINEVA (2017) Dynamic fracture behavior of a nanocrack in a piezoelectric plane. *Zeitschrift für Angewandte Mathematik und Mechanik* **97**(11) 1393-1405.

[15] P. DINEVA, M. MARINOV, T. RANGELOV (2019) Dynamic fracture of a nano-cracked finite exponentially inhomogeneous piezoelectric solid. *Archive of Applied Mechanics* **89** 1317-1332.

[16] P. DINEVA, Y. STOYNOV, T. RANGELOV (2021) Dynamic fracture behavior of nanocracked graded magnetoelectroelastic solid. *Archive of Applied Mechanics* **91** 1495-1508.

[17] I.S. GRADSHTEYN, I.M. RYZHIK (1965) "Tables of Integrals, Series, and Products". Academic Press, New York.

[18] R.G. HOAGLAND, M.S. DAW, J.P. HIRTH (1991) Some aspects of forces and fields in atomic models of crack tips. *Journal of Materials Research* **6** 2565-2571.

[19] A.K. SOH, J.X. LIU (2005) On the constitutive equations of magnitoelectroelastic solids. *Journal of Intelligent Materials Systems and Structures* **16** 597-602.

[20] V.Z. PARTON, B.A. KUDRYAVTSEV (1988) "Electromagnetoelasticity". Gordon and Breach Sci. Publ., New York.

[21] P. DINEVA, D. GROSS, R. MÜLLER, T. RANGELOV (2014) "Dynamic Fracture of Piezoelectric Materials. Solutions of Time-harmonic problems via BIEM". Solid Mechanics and its Applications, v. 212, Springer Int. Publ., Switzerland.

[22] T.A. CRUSE (1978) Two-dimensional BIE fracture mechanics analysis. *Applied Mathematical Modelling* **2** 287-293.

[23] J. SLADEK, V. SLADEK (1987) A BIEM for dynamic crack problems. *Engineering Fracture Mechanics* **27** 269-277.

[24] C. ZHANG, D. GROSS (1998) "On Wave Propagation in Elastic Solids with Cracks". Comput. Mech. Publ., Southampton.

[25] V. VLADIMIROV (1971) "Equations of Mathematical Physics". Marcel Dekker, Inc., New York.

[26] (2007) "Mathematica 6.0 for MS Windows". Champaign, Illinois.

[27] R.K.L. SU, H.Y. SUN (2003) Numerical solution of two–dimensional anisotropic crack problems. *International Journal of Solids and Structures* **40** 4615-4635.

[28] X.F. LI (2005) Dynamic analysis of a cracked magneto-electro-elastic medium under anti-plane mechanical and in-plane electric and magnetic impacts. *International Journal of Solids and Structures* **42** 3185-3205.

[29] V.B. SHENOY (2002) Size-dependent rigidities of nanosized torsional elements. *International Journal of Solids and Structures* **39** 4039-4052.